Parametric Behavior of the Density Profile in the Scrape-off Layer of ASDEX for Neutral-Beam-Heated Plasmas in the L-Regime

K. McCormick, Z.A. Pietrzyk[4], H. Murmann and G. Becker, H.S. Bosch, H. Brocken, A. Carlson, A. Eberhagen, G. Dodel[1], H.-U. Fahrbach, G. Fussmann, O. Gehre, J. Gernhardt, G. v.Gierke, E. Glock, O. Gruber, G. Haas, W. Herrmann, J. Hofmann, A. Izvozchikov[2], E. Holzhauer[1], K. Hübner[3], G. Janeschitz, F. Karger, M. Kaufmann, O. Klüber, M. Kornherr, K. Lackner, M. Lenoci, G. Lisitano, F. Mast, H.M. Mayer, K. McCormick, D. Meisel, V. Mertens, E.R. Müller, J. Neuhauser, H. Niedermeyer, W. Poschenrieder, H. Rapp, A. Rudy, F. Schneider, C. Setzensack, G. Siller, E. Speth, F. Söldner, K. Steinmetz, K.-H. Steuer, N. Tsois[5], S. Ugniewski[6], O. Vollmer, F. Wagner, D. Zasche

Max-Planck-Institut für Plasmaphysik,
EURATOM Association, Garching, FRG

Abstract: Characterizing the scrape-off layer (SOL) density profile by the density at the separatrix n_s and the e-folding length λ_n, the SOL is described for a wide variety of conditions: $\bar{n}_e$=1-5x10^{13} cm^{-3}, I_p=250-440 kA, B_t~22 kG, q_a=2.4-4.3 for injected powers P_{NI}~0.4-1.7 MW, which lead to L-type discharges. Generally, λ_n increases with P_{NI}, these changes becoming more dramatic for lower I_p and $\bar{n}_e$. For OH and NI plasmas n_s is roughly proportional to $\bar{n}_e$; the constant of proportionality increases with NI and is independent of P_{NI} over the range investigated.

Introduction: This paper is designed to furnish an initial data base for the critical evaluation of SOL models, as well as to investigate the premise that the SOL behavior during NI reflects global plasma transport properties as has been observed elsewhere /1, 2/. Statements are limited to the SOL n_e profile in the outer midplane of doubly-null diverted discharges sustained by gas puffing. The ASDEX neutral lithium-beam probe /3, 4/ is used to determine λ_n and the relative changes in n_s; previous experience gained with the edge Thomson scattering system /5/ furnishes an approximate absolute calibration of n_s.

To place matters in context, fig. 1a illustrates the effect of high power (2.75 MW) $H^o \rightarrow D^+$ injection on $\bar{n}_e$, $\beta_{p\perp}$ (taken from the diamagnetic loop) and D_α as well as the Li-beam light signal outside the separatrix. $\bar{n}_e$ decreases going into the L-phase, followed by the H-phase increase and subsequent clamping correlated with the D_α bursts. The characteristic D_α signatures are closely paralled by Li[2p-2s](~ proportional to n_e) /3/. The SOL n_e profiles for OH, L and H (fig. 1b) indicate that $n_s^L<n_s^{OH}<n_s^H$. Further, λ_n^{OH}~1.95 cm, λ_n^L~2.8 cm and λ_n^H~1.1 cm. T_{es}~70, 130 and 250 eV for the OH, L and H-regimes respectively /5/. R-R_s is the distance from separatrix; R_s is derived from magnetic signals and underlies an uncertainty of perhaps 1 cm. This has an important bearing on scaling statements made about n_s; thus if R_s were in fact one cm further outwards, then $n_s^{OH}>n_s^L$~n_s^H would be deduced.

[1] University of Stuttgart; [2] Ioffe Institute; [3] University of Heidelberg; [4] University of Washington, Seattle, USA; [5] N.R.C.N.S. "Democritos", Athens, Greece; [6] Inst. for Nuclear Research, Swierk, Poland;

Results: Fig. 2b depicts for $H^o \to He^{2+}$ injection, λ_n vs. the total absorbed input power $P_{TOT}=P_{OH}+P_{NI}^{abs}$ for $\bar{n}_e=1-4.9\times10^{13}$ cm^{-3} and I_p=420 kA; the energy confinement time "τ_E" deduced from the steady-state NI phase using $\beta_{p\perp}$ to determine the total energy W and "τ_E"=W/P_{TOT} (without correction for radiation effects) is plotted vs. $P_{TOT}/\bar{n}_e$ in fig. 2a.

Fig. 2b demonstrates that during OH (corresponding to the points at the left as in fig. 2a) λ_n is about constant for $\bar{n}_e>1.9\times10^{13}$ cm^{-3}, and is much larger for lower $\bar{n}_e$, as has been previously reported /6/. Auxiliary heating leads to an increase in λ_n, the changes becoming more apparent for lower $\bar{n}_e$ and higher P_{TOT}, τ_E decreases with $P_{TOT}/\bar{n}_e$. Thus, at $\bar{n}_e$ = 4×10^{13} cm^{-3} (1.9×10^{13} cm^{-3}), over the power range λ_n increases by ~10% (22%) and τ_E goes from ~100 to 50 ms (63→45 ms). n_s exhibits the interesting behavior that it is described by an offset-linear law of the form $n_s=a\bar{n}_e+b$, the constants depending only on the type of heating (OH or NI). No parametrical dependence of n_s on P_{NI} is evident; however, for higher P_{NI} a relationship must exist, as documented in fig. 1b where n_s is reduced rather than increased in the L-phase for P_{NI} = 2.85 MW.

The $H^o \to D^+$ series of fig. 3 involve a q_a-(I_p=270-420 kA) and $\bar{n}_e$-scan (2.2, 3.5×10^{13} cm^{-3}). For any given q_a the NI-induced changes in λ_n (see fig. 3b) have the same qualitative behavior as for He: lower $\bar{n}_e$ and higher P_{NI} are both conducive to large alterations in λ_n. The slope of the λ_n vs. q_a curves is about the same for all conditions. With respect to τ_E, for injection with 4 sources τ_E is the same for $\bar{n}_e$=2.2 or 3.5×10^{13} cm^{-3}, whereas λ_n increases by 25% ($\bar{n}_e$ = $2.2\to3.5\times10^{13}$ cm^{-3}), demonstrating that λ_n does not necessarily mirror changes only in τ_E.

In fig. 3c there is no convincing dependence of n_s on q_a; also, the largest absolute δn_s is small, of the order -0.15×10^{13} cm^{-3}. Nevertheless, a plot of n_s vs. $\bar{n}_e$ (not shown here) also reveals an offset-linear relationship, switching from one slope to another as with He, depending on the type of heating used.

Fig. 4 shows the results of another $H^o \to D^+$ power scan with either $\bar{n}_e$ (fig. 4b,c) or I_p (fig. 4d, e) being held constant. The familiar variation of λ_n with P_{NI} and $\bar{n}_e$ is again found, but the changes are more extreme. For example, at $\bar{n}_e$~3×10^{13} cm^{-3} and q_a=4.3 (fig. 4d), λ_n varies from 2.8 to 4.3 cm for P_{TOT}~0.25 → 1.2 MW. In addition, the λ_n^{OH} values are larger than those normally observed on ASDEX by ~0.5 cm. n_s^{NI} clearly increases more strongly with $\bar{n}_e$ for q_a=4.3 than for n_s^{NI}(He) at q_a=2.4 of fig. 2c; on the other hand, the n_s^{OH} values are nearly identical.

Discussion and Summary: It is a common feature of NI-heated plasmas in the L-regime that λ_n increases with P_{NI}, the increase being less pronounced for higher $\bar{n}_e$, and possibly higher I_p. In any case for both OH and NI, λ_n is augmented with q_a: The OH λ_n-q_a scaling of fig. 3b agrees well with previous results /6/, whereas λ_n^{OH} of fig. 4b and 4d is anomalously large for a D^+ plasma. This may be indicative of a deviant wall-conditioning of the divertor. Also, "τ_E" for the series of fig. 4 is noticibly lower. Hence, this series should be regarded in a more qualitative manner.

Whereas it is true that a degradation in τ_E is accompanied by larger λ_n, the reverse conclusion that larger λ_n are synonymous with lower τ_E cannot be universely drawn. It appears that the NI-induced degradation in the cross-field diffusion coefficient $D_\perp$ also extends into the SOL, but that this is only one component in determining λ_n. With respect to τ_E, plotting vs $P_{TOT}/\bar{n}_e$ leads to a surprisingly orderly unification of the OH and NI values, at least for this limited data set. Further, the τ_E scalings for He^{++} of fig. 2a and D^+ of fig. 3a are virtually identical, and of the form $\tau_E \sim \alpha(P_{TOT}/\bar{n}_e)^{-\beta}$ msec (α = 31-32.3, β=0.48, 0.51).

For n_s vs. $\bar{n}_e$, a very clear feature which emerges is that the OH offset-linear scaling switches promptly to a steeper gradient upon initiation of NI, but beyond that shows no dependence on the magnitude of P_{NI}. Higher I_p might bring the OH and NI scalings closer together (compare fig. 2c and 4e): the data base is too small to allow definitive conclusions. As a comment, one of the quantities which should determine n_s for high recycling is the specific heat flux $q_{\parallel}$ into the divertor /7/, which is related to P_{TOT}, λ_n and λ_{Te}. λ_{Te} decreases ~10% /5/ over the P_{NI} range studied here, in contrast to the moderate (at low q_a and high $\bar{n}_e$) 10-20% enhancement in λ_n; therefore $q_{\parallel}$ should increase almost proportionately to P_{TOT}.

No Thomson data was available to calibrate the relative Li-beam determinations of n_s; to obtain n_s absolutely, experience from cross-calibrations of other series were used. Hence, strictly speaking, all absolute n_s values are provisional including the n_s vs. $\bar{n}_e$ scalings. Definitive conclusions can be drawn only with respect to the relative behavior of the switch in scaling between OH and NI discharges. λ_n is generally measured to an accuracy of ±0.1 cm .

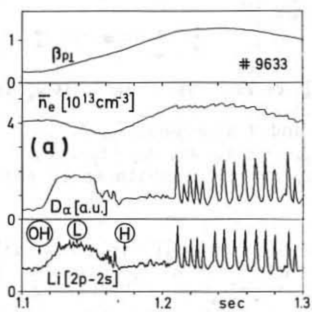

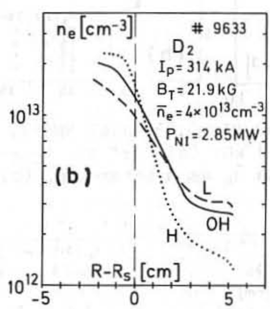

Fig.1 (a) Time behavior of $\beta_{p\perp}$, $\bar{n}_e$, D_α radiation in the divertor and the Li[2p-2s] light intensity several cm outside the separatrix, (b) n_e profiles for the OH, L and H-phases.

References

/1/ F. Wagner, Nucl. Fusion 25 (1985) 525.

/2/ F. Wagner, O. Gruber, et al. 12th EPS (Budapest 1985) 335.

/3/ K. McCormick, H. Murmann and El Shaer, J. Nucl. Mater. 121 (1984) 48.

/4/ K. McCormick, Rev. Sci. Instr. 56 (1985) 1063.

/5/ H. Murmann and M. Huang, Plasma Phys. 27 (1985) 103.

/6/ K. McCormick, Z.A. Pietrzyk, et al., J. Nucl. Mater. 145-147 (1987) 215.

/7/ J. Neuhauser and R. Wunderlich, in ref. /6/ (1987) 877.

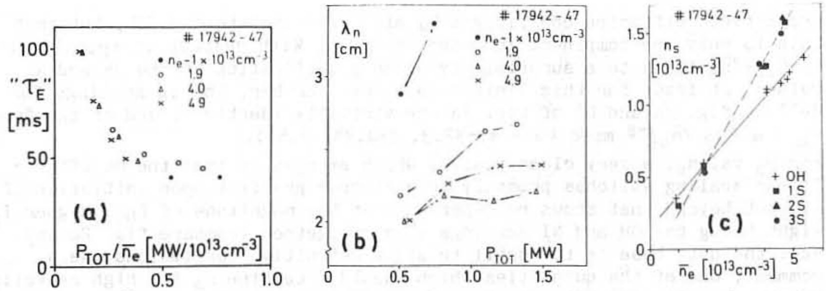

Fig.2 $H^o \rightarrow He^{2+}$ with P_{NI}=0.41, 0.88, 1.24 MW (1, 2 and 3 NI sources), I_p=420 kA, B_t=21.7 kG: (a) energy confinement time "τ_E" vs. $P_{TOT}/\bar{n}_e$, (b) density e-folding length λ_n in the SOL vs. P_{TOT} with $\bar{n}_e$ as a parameter. (c) Separatrix density n_s vs. $\bar{n}_e$ during OH and NI.

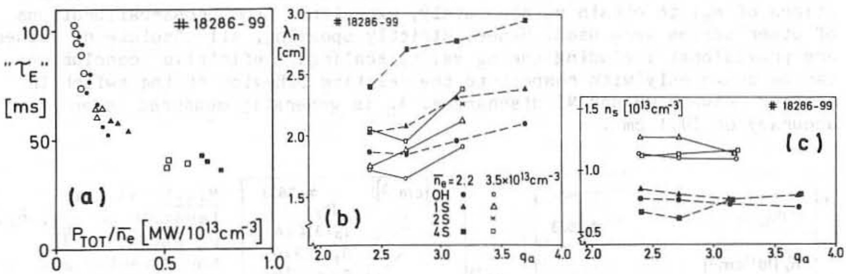

Fig.3 $H^o \rightarrow D^+$ with P_{NI}=0.41, 0.83, 1.67 MW (1, 2 and 4 sources), $\bar{n}_e$=2.2, 3.5×10^{13} cm^{-3}, B_t=21.8 kG: (a) "τ_E" vs. $P_{TOT}/\bar{n}_e$, (b) λ_n vs. q_a (I_p=270, 320, 370, 420 kA) with $\bar{n}_e$ as a parameter, (c) n_s vs. q_a, symbols as in (b).

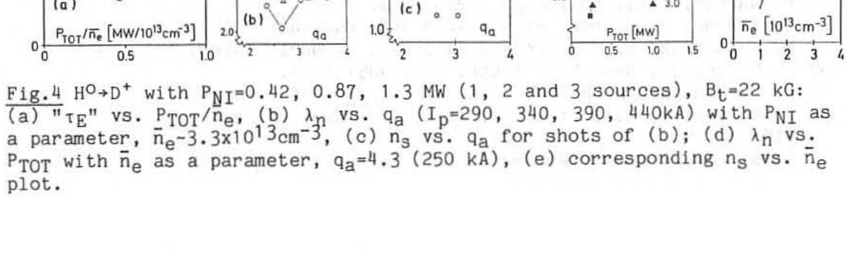

Fig.4 $H^o \rightarrow D^+$ with P_{NI}=0.42, 0.87, 1.3 MW (1, 2 and 3 sources), B_t=22 kG: (a) "τ_E" vs. $P_{TOT}/\bar{n}_e$, (b) λ_n vs. q_a (I_p=290, 340, 390, 440kA) with P_{NI} as a parameter, $\bar{n}_e$~3.3×10^{13}cm^{-3}, (c) n_s vs. q_a for shots of (b); (d) λ_n vs. P_{TOT} with $\bar{n}_e$ as a parameter, q_a=4.3 (250 kA), (e) corresponding n_s vs. $\bar{n}_e$ plot.